HHS Public Access

Author manuscript

J Mol Biochem. Author manuscript; available in PMC 2019 May 21.

Published in final edited form as:

J Mol Biochem. 2018 ; 7: 48–59.

Adenylyl cyclases and TRPV4 mediate Ca^{2+}/cAMP dynamics to enhance fluid flow-induced osteogenesis in osteocytes

Emily R Moore, **Han Seul Ryu**, **Ya Xing Zhu**, and **Christopher R Jacobs**

Columbia University, New York, NY, USA

Abstract

Bone adapts to physical forces and this process is dependent on osteocyte mechanotransduction. One way osteocytes sense mechanical stimulation is through the primary cilium, a sensory organelle that triggers intracellular signaling cascades in response to fluid shear. Our lab previously determined that flow-induced ciliary Ca^{2+} influx and changes in cytosolic cAMP levels are critical for osteogenesis. We also identified two proteins important for osteocyte mechanotransduction: transient receptor potential vanilloid 4 (TRPV4) and adenylyl cyclase 6 (AC6). Interestingly, disrupting the Ca^{2+}-binding ability of these proteins results in loss of function. Although knockdowns of TRPV4 and AC6 disrupt osteogenesis, there is no definitive evidence linking them to Ca^{2+}/cAMP dynamics that facilitate osteocyte mechanotransduction. We therefore transfected MLO-Y4 osteocytes with AC3/6 and TRPV4 overexpression plasmids that fail to interact with Ca^{2+} and observed the response to fluid shear. Indeed, mutant groups exhibited adverse changes in cAMP and lower mRNA expression of an osteogenic marker, COX-2, at the onset of flow. This pattern persisted for AC3 and TRPV4 but we detected no difference in AC6 at longer exposure to flow. These results suggest TRPV4 and ACs mediate Ca^{2+}/cAMP dynamics that are important for osteocyte mechanotransduction. These mechanisms are potential targets for therapeutics to combat bone loss and should be investigated further.

Introduction

One scenario in which the adult skeleton adapts to external stimulation is by generating more bone in response to heightened forces. This load-induced bone formation appears to be coordinated by osteocytes, the sensory cells in bone that serve as signaling centers for osteogenesis. Skeletal maintenance and adaptation is therefore dependent on osteocyte mechanotransduction, or the process of converting physical stimulation into intracellular signaling cascades. Osteocytes are embedded in cortical bone, residing in fluid-filled pockets (lacunae) connected via microscopic channels (canaliculi). One prevailing theory for osteocyte mechanotransduction proposes that physical loading generates fluid flow through

Correspondence should be addressed to Emily R Moore; Phone: +1 330 280 2353, erm17@case.edu.

Author Contributions

Concept and design of experiments: ERM and CRJ. Funding and oversight: CRJ. Data collection: ERM, HSR, YXZ. Data analysis: ERM, CRJ, HSR, YXZ. Figure design: ERM, HSR, YXZ. Original manuscript: ERM and HSR. Manuscript edits: ERM, HSR, and CRJ.

Conflicts of interest

The authors declare no conflicts of interest.

the lacunar/canalicular system, resulting in shear stresses that act on osteocytes. In this model it is believed that fluid shear triggers activation of osteogenic pathways within the osteocyte, but the exact mechanisms required for osteocyte stimulation remain an important open question.

One mechanism by which osteocytes transduce mechanical stimuli is through the primary cilium, a solitary sensory organelle that projects from the cell surface. The primary cilium bends in response to fluid shear *in vitro* and contains a unique microdomain of proteins and signaling molecules that enhance mechanotransduction. For example, the predominant model for kidney cilia exposed to fluid flow is that the cilium bends and calcium (Ca^{2+}) enters the cilium through a transmembrane protein, polycystin 1 (PC1), interacting with a Ca^{2+} channel, polycystin 2 (PC2). Our lab recently determined that osteocyte primary cilia experience a similar flow-induced Ca^{2+} influx and this is critical to osteogenesis, a cellular response that eventually elicits bone formation. However, osteocyte ciliary Ca^{2+} influx does not occur through the PC1/PC2 complex (Lee *et al.* 2015). We previously identified another Ca^{2+} channel, Transient Receptor Potential Vanilloid 4 (TRPV4), is present in the osteocyte cilium and knockdown of TRPV4 attenuates flow-induced osteogenesis (Lee *et al.* 2015). TRV4 is also highly expressed in the primary cilium of mesenchymal stem cells (MSCs) and necessary for fluid shear-induced calcium signaling and subsequent osteogenic gene expression in these cells (Corrigan *et al.* 2018). Interestingly, MSCs lacking primary cilia were unresponsive to pharmacological activation of TRPV4 that was found to enhance osteogenesis (Corrigan *et al.* 2018). We therefore speculate that, in response to fluid shear, Ca^{2+} perhaps enters the osteocyte cilium through the opening of TRPV4 channels.

Previous studies have established that TRPV4 must bind Ca^{2+} to activate intracellular Ca^{2+} influx, a process that is critical to the function of bone cells. Strotmann et al. initially determined that TRPV4 is potentiated by Ca^{2+} interacting with a C-terminal calcium-modulated protein – known as Calmodulin (CaM) domain (Strotmann *et al.* 2003). When this CaM domain is removed, TRPV4-mediated Ca^{2+} entry does not occur. Another group implemented this mutation and determined that osteoclasts, which are activated to resorb bone, remained inactive *in vitro* when the CaM domain was absent (Masuyama *et al.* 2008). Moreover, mice containing this mutation demonstrated enhanced bone formation *in vivo* due to attenuated osteoclast activation (Masuyama *et al.* 2012). A recent study proposed that fluid shear initiates osteocyte mechanotransduction in a microtubule-dependent mechanism involving TRPV4-mediated Ca^{2+} entry (Lyons *et al.* 2017). Combined with the aforementioned experiments in MSCs, these studies suggest TRPV4 interacts with Ca^{2+} to trigger Ca^{2+}-mediated intracellular signaling and can potentially be pharmacologically targeted to enhance osteogenesis.

A second key difference from kidney cells is that osteocyte primary cilia contain unique adenylyl cyclases (ACs). ACs convert ATP to cyclic AMP (cAMP), a signaling molecule that is downregulated in osteocytes at the onset of fluid shear and elevated for longer durations of flow (Kwon *et al.* 2010). There are nine transmembrane isoforms of AC but only AC6 is believed to localize to the osteocyte cilium and is not found in kidney cilia (Kwon *et al.* 2010). We previously demonstrated that osteocytes containing siRNA-mediated knockdowns of AC6 maintained cytosolic levels of cAMP with fluid shear, resulting in

attenuated osteogenesis (Kwon *et al.* 2010). This finding is consistent with osteocytes containing an siRNA-mediated knockdown of Ift88, a protein critical for cilium presence and function. Furthermore, transgenic mice with a global knockout of AC6 exhibit attenuated load-induced bone formation (Lee *et al.* 2014) similar to mice lacking primary cilia in osteoblasts, also known as bone-forming cells (Temiyasathit *et al.* 2012). Interestingly, AC6-mediated production of cAMP is inhibited by Ca^{2+}, whereas other ACs, such as AC3, are activated by Ca^{2+} to produce cAMP (Halls & Cooper 2011). Initial decreases in cAMP production can perhaps be attributed to Ca^{2+} inhibition of AC6, but the eventual increase in cAMP levels alludes to a separate mechanism, such as Ca^{2+}-excitable AC3. Despite the building evidence correlating Ca^{2+} and cAMP dynamics in the cilium, there is no definitive evidence or mechanism to link the two.

TRPV4, AC3, and AC6 all contain Ca^{2+} binding domains that can be disrupted through genetic mutations. Extracellular Ca^{2+} binds to a calcium-modulated protein (calmodulin, CaM) domain of TRPV4, causing this channel to open and trigger Ca^{2+} entry in the cell (Strotmann *et al.* 2003). This CaM domain can be removed by eliminating 17 residues without disrupting general TRPV4 function (Strotmann *et al.* 2003). Indeed, this mutation was found to inhibit calcium influx in and subsequent activation of osteoclasts, the cells responsible for removing bone (Masuyama *et al.* 2012). Protein binding experiments revealed that AC5 competitively binds Ca^{2+} via a domain conserved between AC5 and AC6, and its ability to produce cAMP is inhibited in the bound state (Hu *et al.* 2002). Another group used x-ray crystallography to identify two aspartic acid residues that are critical for AC6 to fold and form the binding pocket (Mou *et al.* 2009). Mutation of these two residues renders AC6 unable to bind calcium and it continues to catalyze the conversion of ATP to cAMP. This binding pocket is conserved in AC3, but is activated by Ca^{2+} to produce cAMP (Halls & Cooper 2011). Thus, in contrast to AC6, disrupting AC3's binding pocket prevents cAMP production. Although these mutations are well defined, they have yet to be explored in the context of the primary cilium or osteocyte mechanotransduction.

Overall, it is largely unknown how Ca^{2+} and cAMP operate in the primary cilium and what role, if any, AC6 plays in mechanotransduction. We hypothesize that fluid flow bends osteocyte primary cilia, triggering Ca^{2+} entry through TRPV4 channels. We further anticipate that in the early initiation of flow, Ca^{2+} binds to AC6 and AC3 to inhibit and enhance production of cAMP, respectively, resulting in upregulation of osteogenic markers. The objectives of this study are to determine whether 1) Ca^{2+}-mediated opening of TRPV4 is critical to osteogenesis and 2) AC6 and AC3 mediate flow-induced Ca^{2+}/cAMP dynamics.

Materials and Methods

Plasmid design and construction

Entry clones for murine AC6 (MmCD00297230) and human AC3 (HsCD00505998) in pENTR223.1 vectors were obtained from the DNASU Plasmid Repository. AC6 and AC3 entry clones were inserted into a pcDNA3.2 mammalian expression destination vector (12489019, Life Technologies) using the Gateway LR Clonase System (Life Technologies) to generate pcDNA3.2 + AC6 (AC6 OE) and pcDNA3.2 + AC3 (AC3 OE) overexpression plasmids. This kit provides a reaction control entry clone, GWCAT, to generate a pcDNA3.2

+ GWCAT overexpression vector. Transfection alone alters normal cell behavior so pcDNA3.2 + GWCAT (Control OE) was used as a control, rather than untransfected cells, for all experiments. All of our pcDNA3.2 plasmids have a V5 tag at the end of the inserted protein.

Mutation of the AC calcium binding pocket has been previously described (Hu *et al.* 2002, Mou *et al.* 2009) and was generated here via site directed mutagenesis. Specifically, we identified the two charged aspartic (Asp) acid residues responsible for calcium binding (Mou *et al.* 2009) and performed point mutations to convert them to neutral alanine (Ala) residues. These residues are located in the 324th and 368th positions for AC3 and the 382nd and 426th positions for AC6. PCR was performed on the AC3 and AC6 OE plasmids using custom designed mutation primers to convert the Asp residues to Ala (Table 1). Resulting PCR product was ligated and transformed using the Q5 Site-Directed Mutagenesis Kit (New England Biolabs). Plasmids were isolated from bacteria using a QIAprep Spin Miniprep Kit (Qiagen). The resulting plasmids are pcDNA3.2 + AC3$^{Ala\ 324,\ 368}$ (AC3 Mut OE) and pcDNA3.2 + AC6$^{Ala\ 382,\ 426}$ (AC6 Mut OE) overexpression plasmids that contain AC3 and AC6 that cannot bind calcium, respectively.

OE plasmid contains TRPV4 flagged with a yellow fluorescent protein (YFP) tag in a pcDNA3.1 vector. Removal of the CaM domain has been previously described (Masuyama *et al.* 2008, 2012) and was generated using the aforementioned site directed mutagenesis protocol with published primer sequences (Masuyama *et al.* 2012). The pcDNA3.1 and pcDNA3.2 vectors have negligible differences that will not affect this experiment; thus, pcDNA3.2 + GWCAT (Control OE) was also used as a vector control for all TRPV4 experiments. All constructed plasmids and sequence mutations were confirmed using Sanger sequencing (Genewiz) and custom primers (Integrated DNA Technologies) (Table 1).

Cell culture

MLO-Y4s were passaged at least twice before used for experiments, seeded on Type I Collagen coated dishes or glass slides, and cultured in MEMα supplemented with 5% FBS, 5% CS, and 1% PenStrep (Life Technologies). Cells were cultured in reduced serum media (MEMα supplemented with 2.5% FBS, 2.5% CS, and 0.5% P/S) 48 hours prior to fluid flow. MLO-Y4s did not reach over 60% confluence in standard passage, but were grown to reach at least 80% confluence for fluid flow studies. Cells transfected with AC6 OE or AC6 Mut OE were cultured in MLOY4 media supplemented with 600 ug/mL Geneticin (Life Technologies) for 48 hours the day after electroporation, followed by 48 hours of reduced serum media. AC3 OE and AC3 Mut OE specimens received reduced serum media for 48 hours the day after electroporation. AC3 and AC6 plasmids were cultured for a total of 3 and 5 days, respectively, before experimentation since this is when each plasmid demonstrated peak protein expression (Figure 1). Passages 38 – 48 were used for all experiments.

Transfections

For each transfection, 1.25 million MLO-Y4s were suspended in 250 μL of BTX Buffer (Harvard Apparatus). Plasmid DNA was added to the cells in BTX solution and gently flicked to mix, then transferred to a 4 mm gap cuvette for electroporation. The amount of

plasmid DNA added was normalized to copy number; therefore, AC3 OE/AC3 Mut OE/AC6 OE/AC6 Mut OE/TRPV4 OE/TRPV4 Mut OE specimens received 15 μg and the GWCAT Control OE group received 7 μg per transfection. Cells were transfected via electroporation using a BTX ECM 360 Electro Cell Manipulator (Harvard Apparatus) to generate a single pulse with settings: 300 V, 100 Ω, 1000 μF. Cells remained in BTX buffer for no more than 10 minutes to minimize cell death. The resulting electroporation solution was split between 4 glass slides for fluid flow studies or 4 100 mm tissue culture dishes for Forskolin treatment. 10 μL of electroporation solution was seeded on 35 mm glass bottom dishes for immunocytochemistry. Cells were rinsed and media was changed the morning after a transfection to remove dead cells.

Forskolin treatment

Transfected cells were cultured to achieve peak protein expression and treated with 10 μM Forskolin (Sigma) dissolved in DMSO (Sigma) or vehicle control for 20 minutes at 37°C. After treatment, cells were lysed using 1 mL of 0.1 M HCl (cAMP ELISA kit, Enzo) for 10 minutes at room temperature and centrifuged at 4°C for 15 min at 16 rcf. The resulting supernatant was transferred to a fresh tube for the cAMP assay.

Immunocytochemistry (ICC)

To determine plasmid expression patterns, double ICC was performed to detect AC3/AC6 and V5 tag of the destination vector. Cells were fixed with 4% paraformaldehyde for 10 min at room temperature and blocked with 3% BSA + 2% goat serum + 0.1% TritonX-100 (Sigma) in PBS for 1 hour at room temperature. Cells were then incubated in primary antibodies against V5 (1:500, Life Technologies) and either AC3 (1:1000, FabGennix) or AC6 (1:1000, abcam) for one hour on a rocker at room temperature. The fluorescent secondary antibodies, Alexa Fluor 488 (1:500, Life Technologies) and AlexaFluor 568 (1:500, Life Technologies) were applied for 1 hour at room temperature to detect V5 and AC3/AC6, respectively. Nuclei were detected using NucBlue ReadyProbes (Life Technologies).

To examine cilia incidence/length, double ICC for V5 and primary cilia was performed. The same procedure was repeated with primary antibodies against V5 (1:500, Life Technologies) and Arl13b (1:1000, Protein Tech), a protein localized to cilia. Cells were then left overnight on a rocker at 4°C, followed by the addition of secondary antibodies. All fluorescent images were collected using an Olympus Fluoview FV1000 confocal microscope and software.

Quantifying cilium incidence and length

At minimum 4 images per dish containing at least 25 nuclei were analyzed to determine the average incidence and length per specimen (dish). Each transfection was performed on 3 separate occasions to evaluate repeatability and consistency between trials. Once cells reached a minimum of 80% confluence, cilium incidence and length were measured manually from confocal stacks using Image J software. Specifically, individual nuclei and their associated cilia (one per nucleus) were identified and the number of cilia was divided by the total number of nuclei to calculate incidence. The individual cilia were then visualized in 3D stacks and length was determined using measurement tools in Image J to

count the number of pixels along the axoneme. Length and incidence were averaged for each image field and considered a sample (n). Investigators were blinded to the groups during the experiment, staining, image acquisition, and post-imaging analysis steps. Quantifications were performed by two investigators to ensure repeatability and accuracy of reported results. Manual quantifications were validated using custom Matlab algorithms for incidence and length intended for lower magnification fields containing hundreds of nuclei.

Oscillatory fluid flow (OFF)

Transfected MLO-Y4s were seeded on glass slides (Fisher Scientific; 75 × 38 × 1 mm). Upon reaching 80% confluence, cells were placed in parallel-plate flow chambers (56 × 24 × 0.28 mm), incubated at 37°C for 30 minutes at rest, and exposed to 2, 5, or 30 minutes of OFF at 1 Hz with a peak shear stress of 10 dyn/cm^2. For RT-qPCR analysis, samples were incubated for 1 hour (2 and 5 min OFF studies) or 30 min (30 min OFF studies) post-flow and were removed from the chambers, rinsed in cold PBS, and lysed immediately with 1 mL TriReagent (Sigma Aldrich) to isolate RNA. For cAMP quantification studies, 0.5 mM of the phosphodiesterase inhibitor 3-isobutyl-1-methylxanthine (IBMX) (Sigma) was added to flow media to prevent cAMP degradation. At the conclusion of flow, samples were rinsed and lysed immediately with 500 μL of 0.1 M HCl (cAMP ELISA kit, Enzo) for 10 minutes. The resulting lysate was centrifuged at 4°C for 15 min at 16 rcf and the supernatant was transferred to a fresh microcentrifuge tube.

mRNA quantification

RT-qPCR was performed to quantify flow-induced changes in Cyclooxygenase-2 (COX-2), an indicator of flow-induced osteogenesis, and *GAPDH*, a housekeeping gene known to maintain consistent mRNA levels, using fluorescent primers (Life Technologies) and an PRISM 7900 (Applied Biosystems). Samples were performed in triplicate and COX-2 was normalized to *GAPDH* expression levels. OFF samples were normalized to static controls to calculate fold change.

cAMP ELISA

Cytosolic cAMP levels were quantified using a kit from Enzo Life Sciences (ADI-900–163). Samples were analyzed in triplicate and prepared according to the manufacturer's instructions for non-acetylated samples in hydrochloric acid lysis buffer. cAMP levels were normalized to total protein content of the lysate, which was determined by a Pierce BCA Protein Assay (Thermo Fisher). OFF samples were normalized to static controls to calculate fold change.

Statistics

It was concluded that data satisfy the requirements of normality and the variance of statistically compared groups was similar. Data were analyzed using a oneway ANOVA followed by Bonferroni post-hoc correction, or a two-tailed student's t-test. Values are reported as mean ± SEM, with $p < 0.05$ considered statistically significant. Sample size was determined to achieve a power of at least 80%.

Results

Transfected MLO-Y4s overexpress TRPV4, AC3, and AC6 protein

We first determined whether our constructed plasmids would result in supranormal levels of AC3, AC6, and TRPV4 protein. For the TRPV4 plasmids, we visualized YFP in live cells and determined that more than 90% of cells overexpressed the protein 3 days post-transfection (PT) (Figure 4.1A). Double ICC for V5 and AC6 revealed that only 20 – 30% of transfected cells overexpressed AC6 3 days PT. We therefore implemented antibiotic selection and achieved 100% efficiency 5 days PT (Figure 4.1B). We repeated these stains on cells transfected with Control OE, AC3 OE, or AC3 Mut OE. For both AC3 plasmids, 80 – 90% of the cells overexpressed AC3 protein 3 days PT (Figure 4.1B). Cells transfected with the Control OE plasmid demonstrated greater than 90% efficiency 3 days PT (Figure 4.1A) and maintained expression for 5 days PT. The mutation plasmids exhibited identical expression patterns as their non-mutated plasmids (data not shown). For these reasons, AC3 and TRPV4 experiments were performed 3 days PT, while AC6 studies were conducted 5 days PT. Moreover, we considered the GWCAT plasmid an acceptable empty vector control at both time points.

AC3 and AC6 catalytic activity is maintained when the calcium binding pocket is disrupted

The catalytic activity of both AC3 and AC6 is sensitive to Ca^{2+}, but all ACs are activated by the AC agonist forskolin at an independent binding site. We therefore treated transfected MLO-Y4s with forskolin to confirm that our mutations do not disrupt general AC activity. Indeed, AC3/6 Mut OE specimens demonstrated increased cAMP levels that were comparable to AC3/6 OE groups, indicating AC activity is preserved (Figure 2). This result importantly confirms that any changes in cAMP production in the mutant groups are direct consequences of disrupting the Ca^{2+} binding pocket. AC activity in MLO-Y4s transfected with AC3/Mut OE plasmids ($p < 0.001$) and AC6/Mut OE plasmids ($p < 0.01$) was elevated compared to the Control OE group, simply because these cells contain more AC protein.

Cilium length increases with overexpression of AC6

Recent work in our lab suggests MLO-Y4s with longer cilia have an enhanced osteogenic response to fluid shear (Spasic & Jacobs, 2017). We therefore sought to determine whether cilium incidence or length increased when these osteocyte ciliary proteins were overexpressed. Interestingly, cilia length increased only with AC6 normal and mutant overexpression (Figure 3). AC3/Mut OE ($p = 0.634$) and TRPV4/Mut OE ($p = 0.133$) elicited no change compared to vector controls. We did not detect any differences in cilium incidence between any of the groups (Supplementary Figure 1).

Disrupting the calcium binding pocket of AC3 and AC6 alters flow-induced cAMP production

We then investigated how cytosolic cAMP levels change when the Ca^{2+} binding pockets of AC3 and AC6 are disrupted. Transfected cells were exposed to 2 min and 30 min of oscillatory fluid flow (OFF), in accordance with our previous work (Kwon *et al.* 2010), and AC OE groups were normalized to Control OE groups. Normally, osteocytes exhibit

decreased levels of cytosolic cAMP production after 2 min of flow. Indeed, cells transfected with AC3 Mut OE produced less cAMP than the AC3 OE group (Figure 4A), whereas the AC6 Mut OE group exhibited increased levels compared to AC6 OE (Figure 5A). We have previously shown that cAMP levels then increase after 30 min of flow (Kwon *et al.*, 2010). After 30 min OFF, the AC3 Mut OE group demonstrated lower cAMP levels compared to AC3 OE (Figure 4B). Interestingly, there was no significant difference between AC6 OE and AC6 Mut OE groups (Figure 5B), which exhibited cAMP levels similar to the Control OE group ($p = 0.116$).

Osteogenesis is attenuated when cAMP production is altered

We then evaluated changes in flow-induced osteogenesis to identify how cAMP production may influence the osteocyte's response to fluid shear. Specifically, we quantified expression of cyclooxygenase-2 (COX-2), a common readout and surrogate for osteocyte osteogenesis. In response to fluid shear, MLO-Y4s normally demonstrate an increase in COX-2 (Hoey *et al.* 2012, Kwon *et al.* 2010). Cells transfected with AC3 Mut OE had enhanced osteogenesis compared to AC3 OE at both timepoints examined (Figure 4C, D). AC6 Mut OE had an attenuated osteogenic response compared to AC6 OE, but only when flow was applied for 2 min (Figure 5C, D). There was no significant difference between AC6 OE and AC6 Mut OE groups, which exhibited COX-2 readouts similar to the Control OE ($p = 0.215$) group with 30 min of flow. Overall, the data indicate that osteocyte osteogenesis is influenced by AC-mediated cytosolic cAMP production.

Osteogenesis is attenuated when the TRPV4 CaM domain is removed

Finally, we investigated changes in flow-induced osteogenesis when intact and mutated TRPV4 are overexpressed. We exposed cells transfected with TRPV4 OE and TRPV4 Mut OE to 5 and 30 min of flow in accordance with timepoints examined in our initial studies (Kwon *et al.* 2010, Lee *et al.* 2015). Regardless of flow duration, cells overexpressing TRPV4 Mut OE had an attenuated response to flow compared to the TRPV4 OE group. Interestingly, MLOY4s transfected with TRPV4 OE had an enhanced COX-2 response compared to the Control OE group ($p < 0.05$).

Discussion

These studies demonstrate, for the first time, that Ca^{2+} and cAMP are perhaps coupled via adenylyl cyclases in osteocytes. AC3 and AC6 have long been known to bind Ca^{2+} to modify cAMP production (Halls & Cooper 2011), but the purpose of this mechanism remains poorly characterized in the context of cell behavior. AC5/6 expression and activity are important for proper heart development and function (Gao *et al.* 2017, Hu *et al.* 2009) and AC5, which is also inhibited by Ca^{2+}, is critical to Ca^{2+}-mediated cardiac regulation (Okumura *et al.* 2003). AC3 is present in many tissue types and known to bind free Ca^{2+} to stimulate cAMP production (Xia *et al.* 1992), but the cellular function of this phenomena remains largely unknown. Our lab previously identified that, in response to fluid flow, mechanotransduction is initiated when Ca^{2+} enters the MLOY4 primary cilium (Lee *et al.* 2015) and cytosolic cAMP levels decrease (Kwon *et al.* 2010). We further demonstrated that an siRNA-mediated knockdown of AC6 inhibits MLO-Y4 osteogenesis (Kwon *et al.* 2010),

and mice containing a global knockout of AC6 exhibit attenuated load-induced bone formation (Lee *et al.* 2014). We therefore suspected that ACs mediate Ca^{2+} entry and subsequent cAMP production in osteocytes. To determine whether ACs associated with the primary cilium mediate Ca^{2+}/cAMP dynamics during osteocyte mechanotransduction, we disrupted the Ca^{2+} binding pocket of AC3/6 and evaluated flow-induced cAMP production and COX-2 expression. Indeed, osteocytes containing disrupted forms of AC3/6 demonstrated conflicting cAMP production compared to their functional counterparts. Furthermore, osteocytes with higher levels of cytosolic cAMP (AC3 OE and AC6 Mut OE) exhibited attenuated flow-induced osteogenesis. Our results suggest AC3 and AC6 are present in the osteocyte and bind Ca^{2+} to mediate cytosolic cAMP production to facilitate mechanotransduction.

Moreover, our data imply cAMP levels can perhaps be tuned to enhance osteocyte osteogenesis. Our previous work suggests that cytosolic cAMP levels decrease at the onset of flow (2 min OFF) and increase after 30 min of OFF (Kwon *et al.* 2010), but we currently observed that COX-2 levels increase for both flow durations (Figures 4–5). Interestingly, the AC3 OE group, which increased cAMP production, had a significantly attenuated osteogenic response compared to the Control OE group after 2 min of OFF ($p < 0.01$). Moreover, COX-2 expression was diminished in the AC3 Mut OE group compared to Control OE ($p < 0.05$) after 30 min OFF. These results are consistent with our prior findings and indicate that decreased cytosolic cAMP levels are important for the initial onset of fluid flow, whereas elevated cAMP production is required for osteogenesis after a longer duration of flow. Although COX-2 levels were slightly elevated in the AC6 OE group after 2 min OFF, overexpressing the AC6 plasmids did not result in any significant changes compared to controls. Our prior work suggests MLO-Y4s normally contain more AC3 than AC6 protein, so these cells are perhaps more sensitive to elevated cytosolic AC3 expression. It is also probable that AC3 OE cells produced more AC protein than AC6 OE cells, given that we achieved the desired efficiency 48 hours faster with the AC3 plasmids. Another possibility is that since AC3 is activated to produce cAMP, whereas AC6 is merely inhibited, the excitatory behavior had a more drastic impact on normal MLO-Y4 cAMP production.

This work also further implicates TRPV4 as the mechanism by which Ca^{2+} enters the osteocyte during mechanotransduction. A recent study established that fluid shear elicits Ca^{2+} influx in osteocytes via TRPV4 and proposed that this Ca^{2+} channel is an important target for enhancing bone quality (Lyons *et al.*, 2017). Moreover, a prior study conducted by our lab revealed that an siRNA-mediated knockdown of TRPV4 uniquely resulted in attenuated osteogenesis in MLOY4s (Lee *et al.* 2015). We also determined that knockdown of PC2, the predominant Ca^{2+} channel in kidney cilia, does not influence osteocyte mechanotransduction. In the work presented here, we showed that MLOY4s with supranormal TRPV4 protein levels had an enhanced osteogenic response at both short and long-term flow exposure. However, when these cells overexpressed TRPV4 that could not facilitate Ca^{2+} entry into the cell or cilium, the enhanced osteogenic response was lost. This phenomena has also been observed in osteoclasts, which require the same TRPV4 CaM domain to be activated for bone resorption (Masuyama *et al.* 2012). Collectively, these results perhaps suggest that overall bone maintenance relies on TRPV4-mediated activation of osteocytes and osteoclasts, which promote and reduce bone formation, respectively. More

importantly, they demonstrate that expression of proteins associated with mechanotransduction can be engineered to influence osteocyte-mediated osteogenesis.

AC6 is an attractive therapeutic target for bone regeneration since it is potentially unique to osteocyte cilia. Our prior work suggests AC6 is the only AC present in the osteocyte cilium and its existence is unique compared to kidney cilia (Kwon *et al.* 2010). Our group and others have also shown that pharmacologically lengthening cilia enhances the cell's response to fluid-flow and this phenomenon is correlated with increased AC6 expression (Besschetnova *et al.* 2010, Spasic & Jacobs 2017). It is unknown how lengthening enhances osteogenesis but one possibility is that more proteins associated with mechanotransduction are available since the cilium is larger. Additionally, the longer axoneme may sense flow more readily and more easily bend to form a stress concentration at its base. In this study, we demonstrated that only MLO-Y4s overexpressing AC6, not AC3 or TRPV4, had longer cilia. This favors the hypothesis that cilia may lengthen due to increased AC6 availability. Although we identified that TRPV4 is potentially the predominant Ca^{2+} channel in osteocytes, TRPV4 is also important for osteoclast activation (Masuyama *et al.* 2008, 2012). Thus, non-targeted therapeutic strategies that manipulate TRPV4 could simultaneously activate bone formation and resorption. Similarly, AC3 is present in many cell types so any manipulation would need to be targeted to avoid negative side effects. Additionally, AC3 overexpression alone influenced osteogenesis. The primary cilium tunes its response to physical stimuli in order to prevent overstimulation (Nguyen *et al.* 2015). This is an important negative-feedback mechanism inherent to cilium function, so therapeutic strategies should not interfere with this adaptation. There is also evidence that AC3 only binds Ca^{2+} after it has been activated in order to enhance cAMP production, but definitive proof is lacking (Halls & Cooper 2011). If this is true, targeting AC3 may not facilitate the ciliary Ca^{2+}/cAMP dynamics critical to mechanotransduction.

Although AC6 did lengthen osteocyte cilia, we did not detect a significant difference in COX-2 expression compared to controls after 2 and 30 min of OFF. In prior studies, cells were stimulated for an hour (Besschetnova *et al.* 2010, Spasic & Jacobs 2017) so increased AC6 expression may require longer flow exposure to impact the cells. It is also possible that our plasmids generated too much cytosolic AC6 protein and interfered with cAMP production or other cellular processes. This contradiction highlights a potential limitation in our study, which is utilizing CMV-driven overexpression plasmids to explore ciliary proteins. Expression vectors conveniently allow for the study of protein alterations in mammalian cells, but overexpressing protein is not always physiologically relevant. More importantly, these vectors stimulate supranormal protein levels in the cytosol, so we are unable to directly observe their function in the primary cilium. Thus, it is possible that overexpressing AC6 specifically in the primary cilium is critical to observe changes in flow-induced COX-2 expression. Despite this limitation, we were still able to demonstrate that ACs mediate Ca^{2+}/cAMP dynamics and subsequent osteogenesis. Our lab recently developed novel ciliumtargeted biosensors that we will next use to specifically characterize Ca^{2+}/cAMP dynamics in the cilium. We intend to combine these biosensors with the now available CRISPR technology to overexpress, mutate, or eliminate AC3, AC6, and TRPV4 specifically in the cilium.

Collectively, the results from this study build on prior work (Kwon *et al.* 2010, Lee *et al.* 2014, 2015, Spasic & Jacobs 2017) to suggest that AC6 and TRPV4 are important for the immediate onset of flow-induced osteocyte mechanotransduction. We now speculate that, when exposed to flow, the osteocyte cilium bends and extracellular Ca^{2+} binds to the CaM domain of TRPV4 (Figure 4–7). TRPV4 then opens and Ca^{2+} enters the cilium, potentially in the direction from the ciliary base to the axoneme tip (Lee *et al.* 2015). Ciliary Ca^{2+} binds to AC6, which is then unable to catalyze the conversion of ATP to cAMP. Consequently, cytosolic cAMP levels decrease since existing cAMP is recruited for flow-induced intracellular signaling and AC6 is inhibited from replenishing cAMP. AC3 is perhaps important at a later stage of fluid flow stimulation, when cAMP levels increase to encourage osteogenesis.

Supplementary Material

Refer to Web version on PubMed Central for supplementary material.

Acknowledgements

We would like to acknowledge our funding sources from the National Institute of Arthritis and Musculoskeletal and Skin Diseases at the National Institutes of Health R01-AR062177 and T32-AR59038. We thank Dr. Heinrich Brinkmeier at the University of Greifswald for gifting the TRPV4 plasmid. We also thank Michael Duffy and Milos Spasic for technical discussions and/or manuscript edits, as well as Bryan Louie for his technical assistance with quantifying cilium incidence and length.

References

Besschetnova TY, Kolpakova-Hart E, Guan Y, Zhou J, Olsen BR & Shah JV 2010 Identification of Signaling Pathways Regulating Primary Cilium Length and Flow -Mediated Adaptation. Curr Biol 20 182–187 [PubMed: 20096584]

Corrigan MA, Johnson GP, Stavenschi E, Riffault M, Labour MN & Hoey DA 2018 TRPV4-mediates oscillatory fluid shear mechanotransduction in mesenchymal stem cells in part via the primary cilium. Sci Rep 8 3824 [PubMed: 29491434]

Gao MH, Lai NC, Giamouridis D, Kim YC, Guo T & Hammond HK 2017 Cardiac-directed expression of a catalytically inactive adenylyl cyclase 6 protects the heart from sustained β-adrenergic stimulation. PLoS One 12 e0181282 [PubMed: 28767701]

Halls ML & Cooper DMF 2011 Regulation by Ca2+-signaling pathways of adenylyl cyclases. Cold Spring Harb Perspect Biol 3 a004143 [PubMed: 21123395]

Hoey DA, Tormey S, Ramcharan S, O'Brien FJ & Jacobs CR 2012 Primary Cilia-Mediated Mechanotransduction in Human Mesenchymal Stem Cells. Stem Cells 30 2561–2570 [PubMed: 22969057]

Hu B, Nakata H, Gu C, De Beer T & Cooper DMF 2002 A Critical Interplay between Ca2+ Inhibition and Activation by Mg2+ of AC5 Revealed by Mutants and Chimeric Constructs. J Biol Chem 277 33139–33147 [PubMed: 12065575]

Hu CL, Chandra R, Ge H, Pain J, Yan L, Babu G, Depre C, Iwatsubo K, Ishikawa Y, Sadoshima J, Vatner SF & Vatner DE 2009 Adenylyl cyclase type 5 protein expression during cardiac development and stress. Am J Physiol Heart Circ Physiol 297 H1776–1782 [PubMed: 19734365]

Kato Y, Windle JJ, Koop BA, Mundy GR & Bonewald LF 2010 Establishment of an Osteocyte-like Cell Line, MLO-Y4. J Bone Miner Res 12 2014–2023

Kwon RY, Temiyasathit S, Tummala P, Quah CC & Jacobs CR 2010 Primary cilium-dependent mechanosensing is mediated by adenylyl cyclase 6 and cyclic AMP in bone cells. FASEB J 24 2859–2868 [PubMed: 20371630]

Lee KL, Guevarra MD, Nguyen AM, Chua MC, Wang Y & Jacobs CR 2015 The primary cilium functions as a mechanical and calcium signaling nexus. Cilia 4 7 [PubMed: 26029358]

Lee KL, Hoey DA, Spasic M, Tang T, Hammond HK & Jacobs CR 2014 Adenylyl cyclase 6 mediates loading-induced bone adaptation in vivo. FASEB J 28 1157–1165 [PubMed: 24277577]

Lyons JS, Joca HC, Law RA, Williams KM, Kerr JP, Shi G, Khairallah RJ, Martin SS, Konstantopoulos K, Ward CW & Stains JP 2017 Microtubules tune mechanotransduction through NOX2 and TRPV4 to decrease sclerostin abundance in osteocytes. Sci Signal 10 eaan5748

Masuyama R, Vriens J, Voets T, Karashima Y, Owsianik G, Vennekens R, Lieben L, Torrekens S, Moermans K, Vanden Bosch A, Bouillon R, Nilius B & Carmeliet G 2008 TRPV4-Mediated Calcium Influx Regulates Terminal Differentiation of Osteoclasts. Cell Metab 8 257–265 [PubMed: 18762026]

Masuyama R, Mizuno A, Komori H, Kajiya H, Uekawa A, Kitaura H, Okabe K, Ohyama K & Komori T 2012 Calcium/calmodulin-signaling supports TRPV4 activation in osteoclasts and regulates bone mass. J Bone Miner Res 27 1708–1721 [PubMed: 22492541]

Mou TC, Masada N, Cooper DMF & Sprang SR 2009 Structural Basis for Inhibition of Mammalian Adenylyl Cyclase by Calcium. Biochemistry 48 3387–3397 [PubMed: 19243146]

Nguyen AM, Young YN & Jacobs CR 2015 The primary cilium is a self-adaptable, integrating nexus for mechanical stimuli and cellular signaling. Biol. Open 4, 1733–1738 [PubMed: 26603473]

Okumura S, Kawabe J, Yatani A, Takagi G, Lee MC, Hong C, Liu J, Takagi I, Sadoshima J, Vatner DE, Vatner SF & Ishikawa Y 2003 Type 5 Adenylyl Cyclase Disruption Alters Not Only Sympathetic But Also Parasympathetic and Calcium-Mediated Cardiac Regulation. Circ Res 93 364–371 [PubMed: 12869393]

Spasic M & Jacobs C 2017 Lengthening primary cilia enhances cellular mechanosensitivity. Eur Cells Mater 33 158–168

Strotmann R, Schultz G & Plant TD 2003 Ca2+-dependent potentiation of the nonselective cation channel TRPV4 is mediated by a C-terminal calmodulin binding site. J Biol Chem 278 26541–26549 [PubMed: 12724311]

Temiyasathit S, Tang WJ, Leucht P, Anderson CT, Monica SD, Castillo AB, Helms JA, Stearns T & Jacobs CR 2012 Mechanosensing by the Primary Cilium: Deletion of Kif3A Reduces Bone Formation Due to Loading. PLoS One 7 e33368 [PubMed: 22428034]

Xia Z, Choi EJ, Wang F & Storm DR 1992 The type III calcium/calmodulin-sensitive adenylyl cyclase is not specific to olfactory sensory neurons. Neurosci Lett 144 173–169

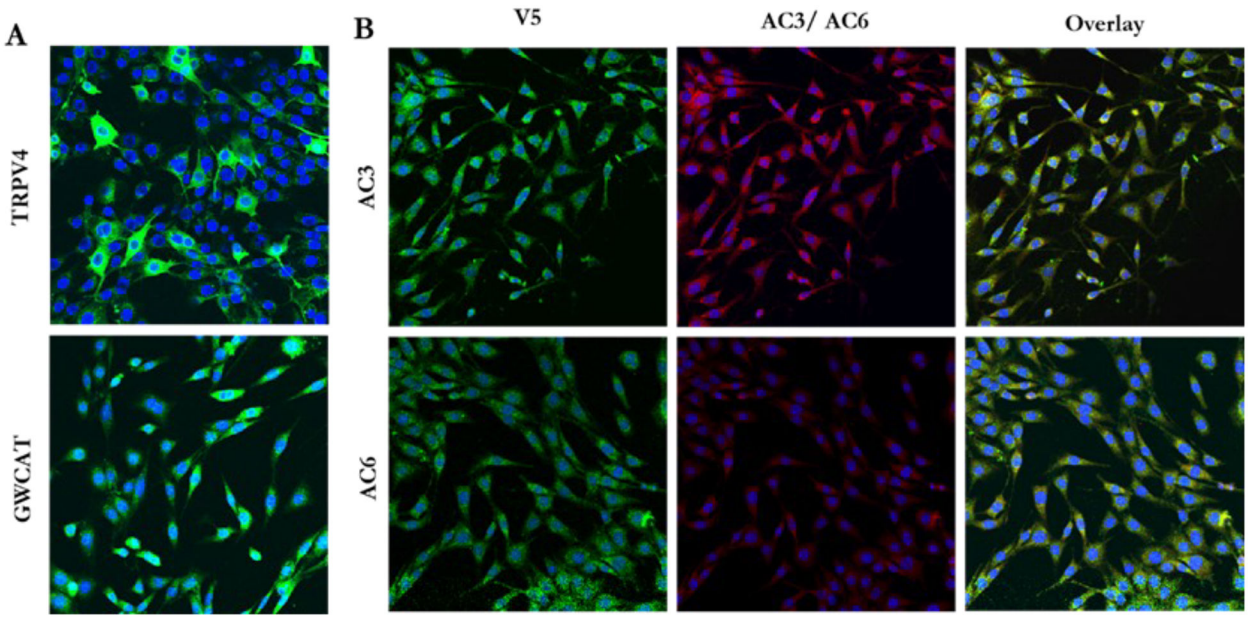

Figure 1.

MLO-Y4s containing our overexpression vectors demonstrate supranormal protein levels. ICC for V5 (green) revealed that MLO-Y4s transfected with GWCAT OE (A, bottom), AC3 OE (B, top), and AC6 OE (B, bottom) overexpress GWCAT, AC3, and AC6 protein, respectively. TRPV4 expression was confirmed by visualizing YFP (green) (A, top). AC3 and AC6 are pictured in red (B, middle). Nuclei are pictured in blue. Images were collected at 20X. This experiment was performed 3 times for each group.

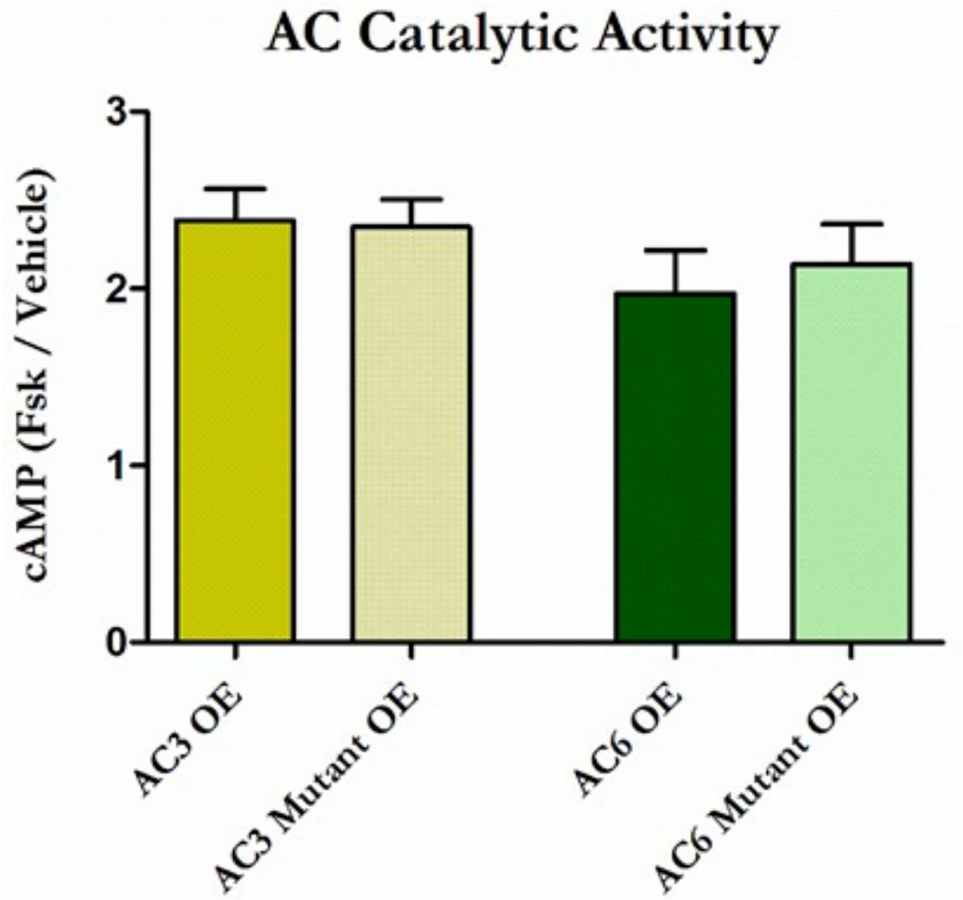

Figure 2.

Ca^{2+} binding pocket disruption does not influence general AC catalytic activity. MLO-Y4s were transfected with AC3 (yellow) and AC6 (green) or their corresponding mutation overexpression plasmids and treated with forskolin. Compared to vehicle controls, all specimens demonstrated an approximate 2-fold increase in cAMP production. This increase was comparable between OE plasmids and their Mut OE counterparts, as well as between AC3 and AC6 specimens. Data are normalized to vehicle controls and reported as the mean ± SEM. n = 5 for AC3 specimens, n = 6 for AC6 specimens. This experiment was performed 3 times for each group.

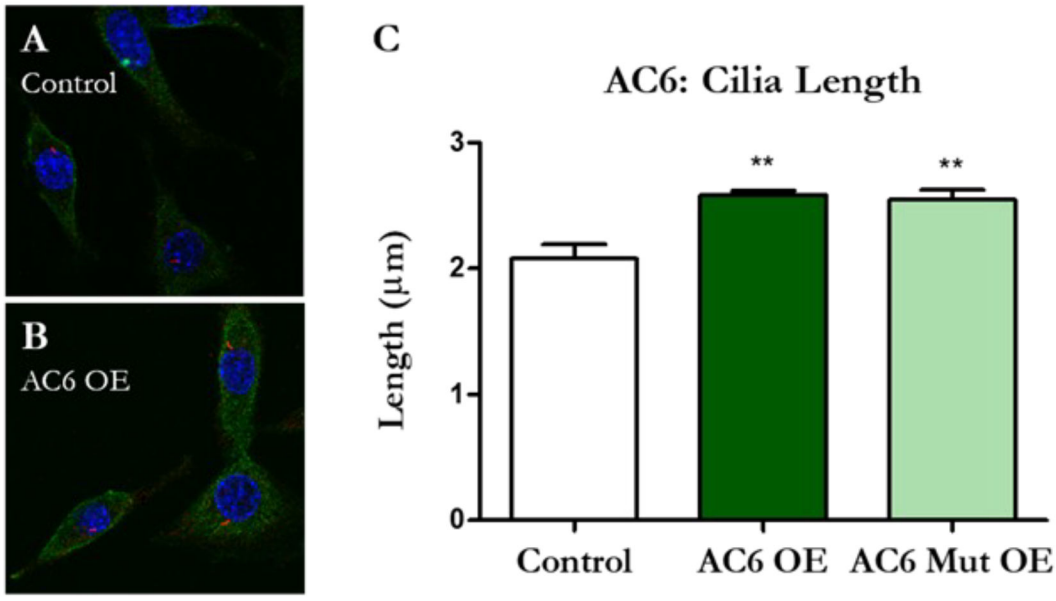

Figure 3.

Osteocyte primary cilia lengthen with increased AC6 protein expression. Cilia were identified in transfected MLO-Y4s using double ICC for V5 (green) and Arl13b, a protein that localizes to cilia (red). Cell nuclei are pictured in blue. Visually, cilia appeared to be longer in AC6 OE (B) and AC6 Mut OE samples (not pictured) compared to Control OE (B). Three dimensional stacks were collected at 100X magnification using a confocal microscope. Cilia incidence and length were measured manually using Image J software. Indeed, AC6 and AC6 Mut OE demonstrated longer cilia (C) but this effect was not present in AC3 and TRPV4 OE samples. Data are presented as mean ± SEM, **$p < 0.001$. Control n = 15, OE n = 12, Mut OE n = 12. This experiment was performed 3 times.

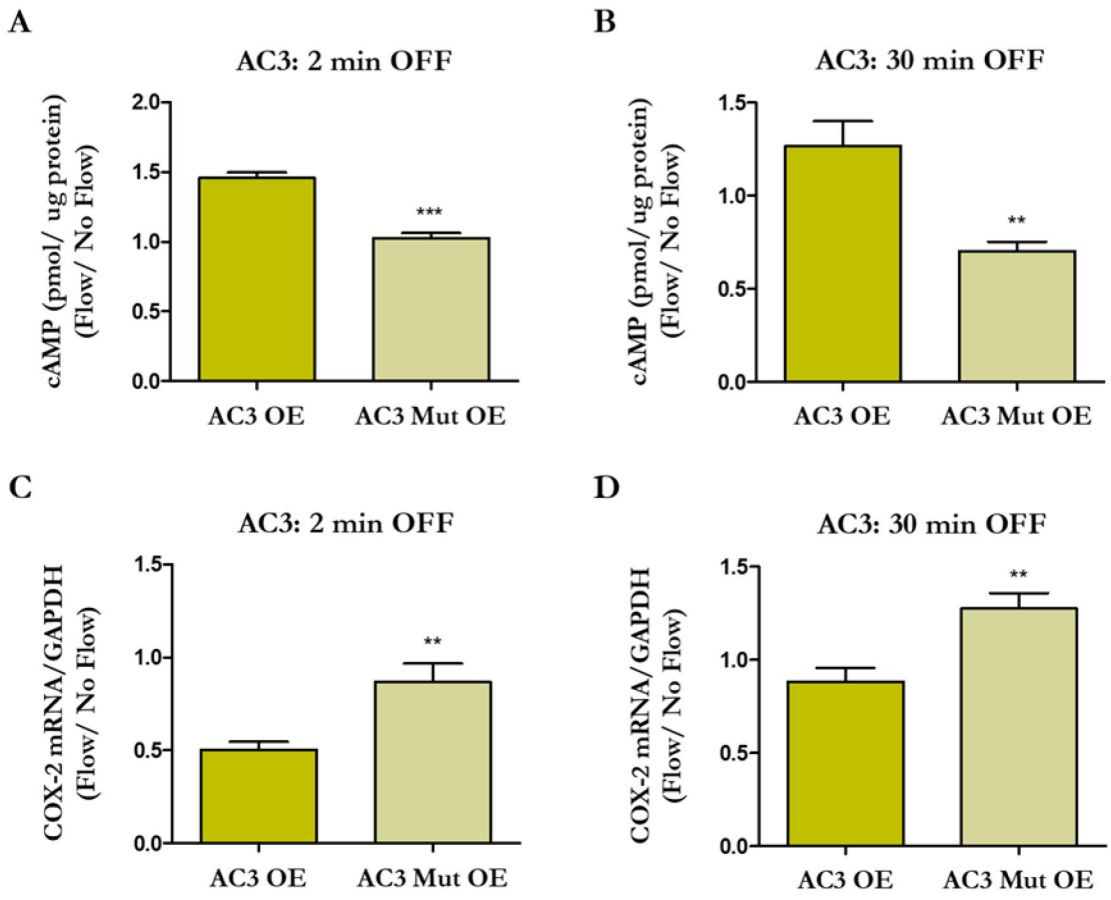

Figure 4.

Flow-induced changes in cAMP levels and COX-2 expression in osteocytes overexpressing intact and mutated AC3. MLO-Y4s were transfected with AC3 OE, AC3 Mut OE, or Control OE plasmids and exposed to 2 or 30 min OFF. The AC3 Mut OE group exhibits decreased cAMP levels (A, B) and enhanced osteogenesis (C, D) compared to AC3 OE. Bar graphs represent fold changes with OFF compared to static controls. AC3 OE and AC3 Mut OE are normalized to Control OE. Data are presented as mean ± SEM. n = 6 for all groups, **$p < 0.001$, ***$p < 0.0001$. These experiments were performed 3 – 4 times for each group.

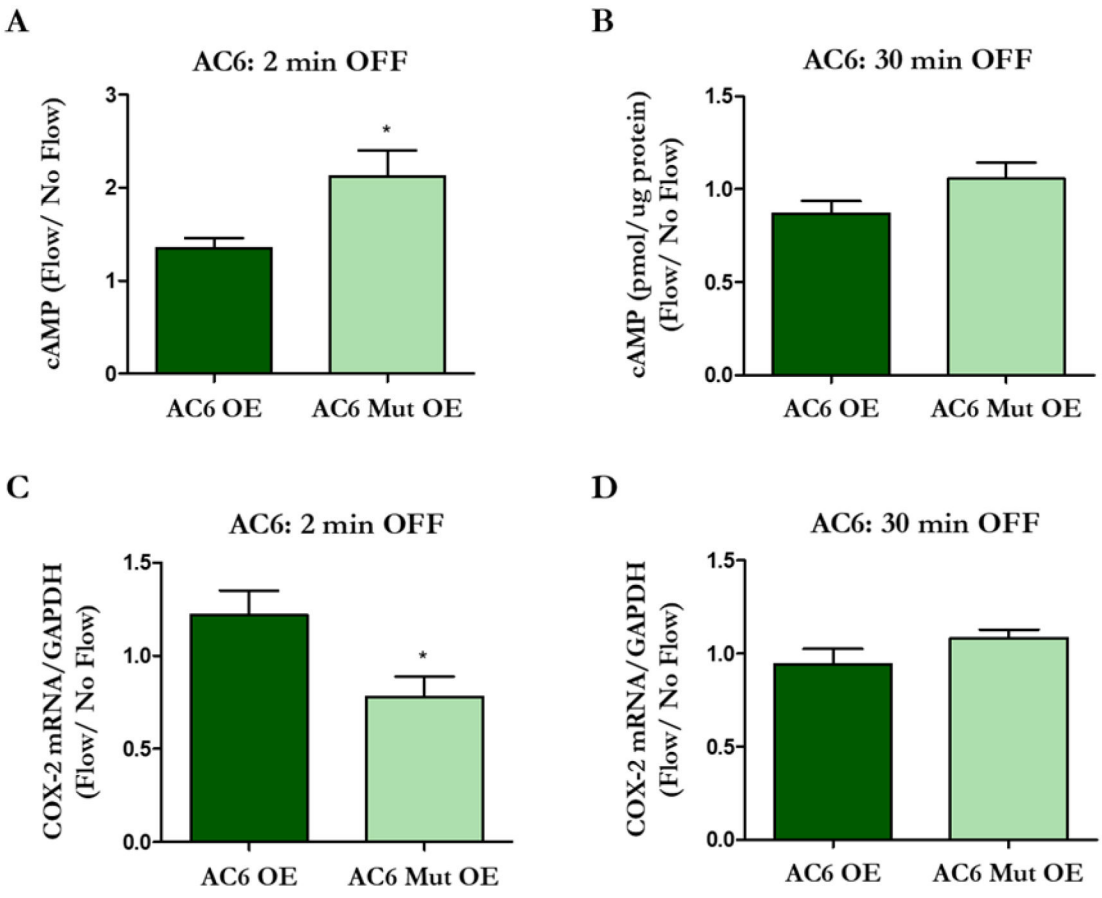

Figure 5.

Flow-induced changes in cAMP levels and COX-2 expression in osteocytes overexpressing intact and mutated AC6. MLO-Y4s were transfected with AC6 OE, AC6 Mut OE, or Control OE plasmids and exposed to 2 or 30 min OFF. After 2 min of OFF, the AC6 Mut OE group exhibits an increase in cAMP production (A) and decreased osteogenic response (C) compared to the AC6 OE group. There is no difference in cAMP production (B) or COX-2 expression (D) between the groups with 30 min of OFF. Bar graphs represented fold changes with OFF compared to static controls. AC6 OE and AC6 Mut OE are normalized to Control OE. Data are presented as mean ± SEM. n = 6 for all groups, *$p < 0.01$. These experiments were repeated 3 times for each group.

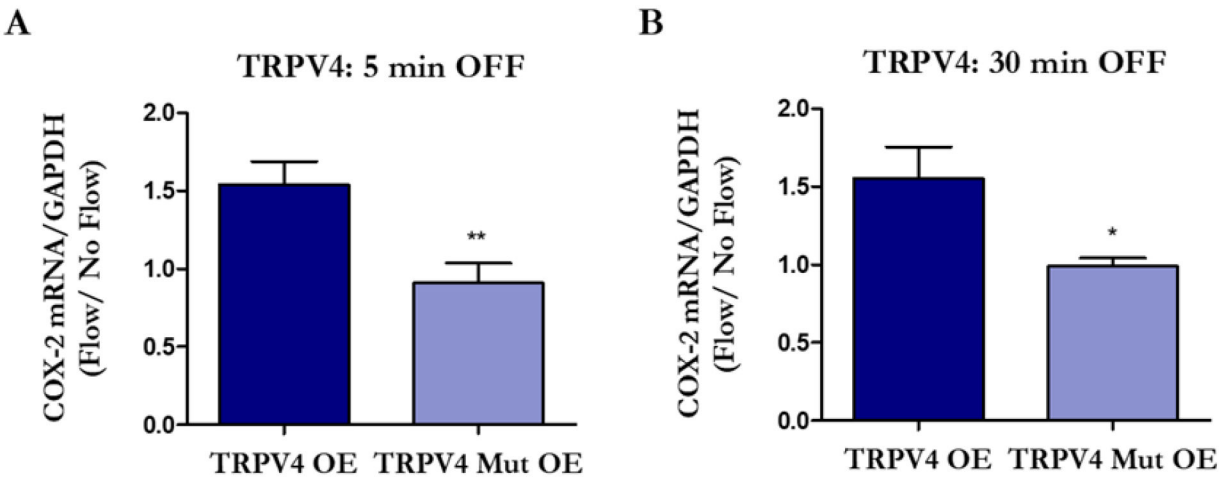

Figure 6.

Osteocytes demonstrate attenuated flow-induced osteogenesis when the CaM domain of TRPV4 is removed. MLOY4s were transfected with TRPV4 OE, TRPV4 Mut OE, or Control OE plasmids and exposed to 5 or 30 min OFF. The TRPV4 Mut OE group has an attenuated COX-2 response compared to the TRPV4 OE group. Bar graphs represented fold changes with OFF compared to static controls. TRPV4 OE and TRPV4 Mut OE data are normalized to Control OE data. Data are presented as mean ± SEM. n = 6 for all groups, *p < 0.01, **p < 0.001. These experiments were performed 3 times for each group.

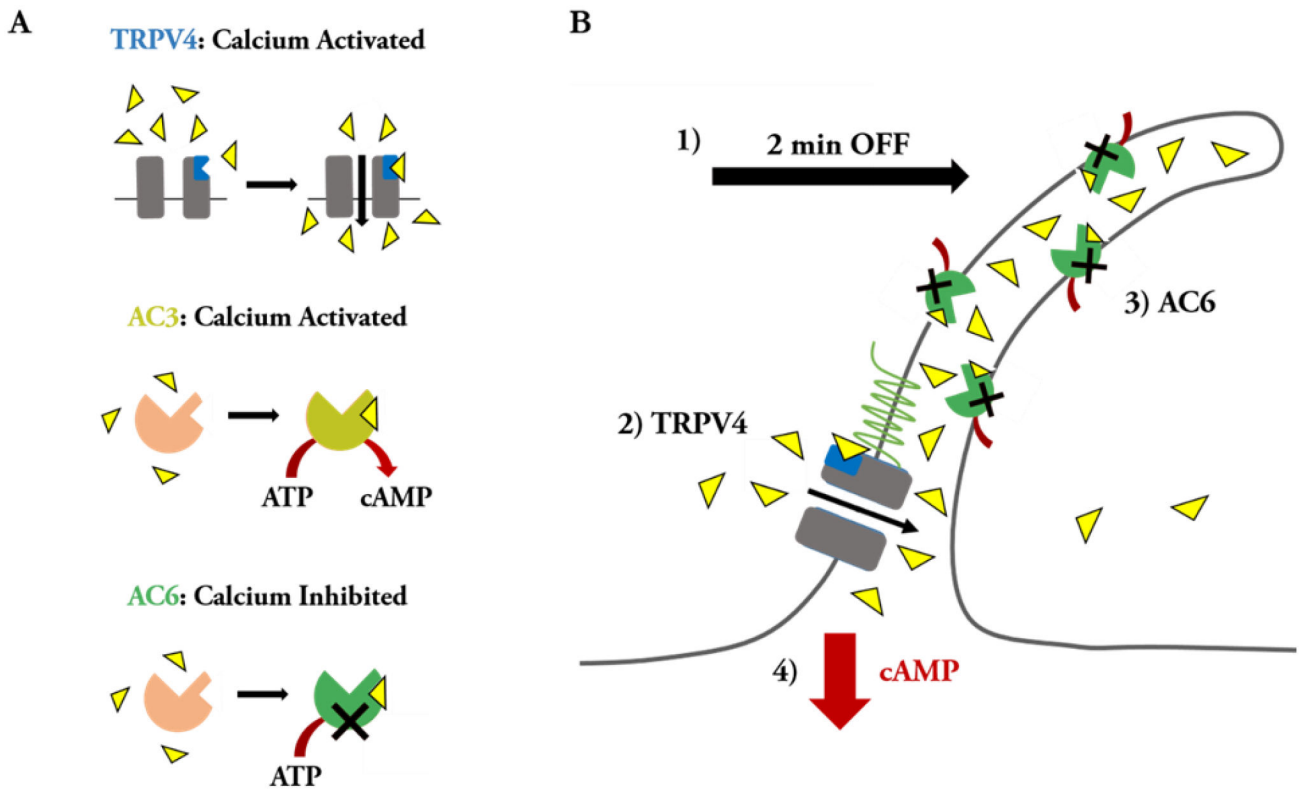

Figure 7.

Proposed Ca^{2+}/cAMP dynamics involving the osteocyte primary cilium microdomain. (A) summary of ciliary proteins and the effects of Ca^{2+} binding. (B) Cartoon depicting our hypothesis of Ca^{2+}/cAMP dynamics in the osteocyte primary cilium. We propose that, in the initial onset of fluid shear, the cilium bends (1) and extracellular Ca^{2+} enters the osteocyte cilium by binding TRPV4 to facilitate opening of this channel, resulting in a ciliary influx of Ca^{2+} (2). The Ca^{2+} that enters the cilium then binds to AC6 (3), inhibiting production of cAMP (4).

Table 1.

Mutation and sequencing primers for mutation plasmid design

Plasmid	Mutation Primers	Sequencing Primer
AC3 Mut OE	324 For: TCCTCTTTGCCGCCATCG 324 Rev: TGCTGACGTTCTCGTGACG 368 For: TTAAGATCCTGGGCGCCTGC 368 Rev: TCCGCAGCTGGTGGTATTTAGC	For: TCTATGACGGTGATGGTGTTCC
AC6 Mut OE	382 For: TTGAGGGCTTCACCAGCCTG 382 Rev: TGGCCGCAAACAGGATGCTG 426 For: TAGGAGCCTGTTACTACTGC 426 Rev: AGATCTTGATCCTCAGACAG	For: TGTCTGCACACACTACCCTG
TRPV4 Mut OE	For: CTTCTCCCTGAACAAGAACTCAAGC Rev: TTGTTCAGGGAGAAGCCATAGTACTG	For: TCTCTACCACTGACACCCGTTC